ION IMPLANTATION APPLIED TO FUSION RESEARCH*

F. L. Vook, B. L. Doyle, and G. T. Picraux
Sandia Laboratories**
Albuquerque, New Mexico 87185

ABSTRACT

Ion implantation and microanalysis have been used to investigate plasma-surface interactions relevant to fusion applications. Previous results for pure metals are reviewed and current results are presented for TiB_2 and B_4C coatings for tokamak surfaces. Enhanced trapping of implanted, low-energy hydrogen has been shown to occur at room temperature in W, Au, Pd, Mo, Nb, TiB_2, and B_4C for He or other ion predamage. Hydrogen depth profiles obtained using $^1H(^{19}F,\alpha\gamma)^{16}O$ resonant nuclear reaction show that the H decorates the He damage profiles at traps whose concentration is proportional to the amount of He-induced damage. For room temperature implantation in TiB_2 and B_4C, H is trapped at the end of range, and isochronal annealing followed by depth profiling indicates that the H is lost by release from traps followed by rapid diffusion. The hydrogen is detrapped from TiB_2 at substantially lower temperatures or laser energy fluxes (pulsed annealing) than for B_4C. For He predamaged samples, annealing at 400°C causes the H to be retrapped in the region of the He-induced damage. On the

*This work was supported by the U.S. Department of Energy under Contract DE-AC04-76-DP00789.

**A U.S. Department of Energy facility.

basis of tritium inventory control, TiB_2 appears to be superior to B_4C. H depth profiling has also been shown to be a useful plasma diagnostic technique for the measurement of particle and flux energy distributions near the wall. These measurements have been used to determine the plasma edge temperatures as a function of distance from the plasma in an operating tokamak.

I. INTRODUCTION

Ion implantation and ion microanalysis increasingly are being used to analyze the interaction of light elements such as helium and hydrogen with the near surfaces of solids. Such studies are especially important in fusion materials research where the understanding of plasma-surface interactions is particularly important to the achievement of continued progress in fusion technology. Two major current problems are the understanding and control of hydrogen trapping and recycle at first-wall surfaces and the minimization of contamination of the plasma from impurities emitted from interior surfaces. A recent thrust in impurity control is the development of low-Z coatings for high-power tokamak surfaces, such as limiters.

The first requirement of such limiters, or other first-wall components, is the ability to survive repeated high-energy deposition pulsing.[1] Primary problems are keeping the component's temperature below the melting temperature and preventing destructive thermal shocks which can be caused by intense beams of electrons, ions, and neutrals. It has also been well documented that the

limiter constitutes a major source of impurities in the discharge plasma.[2] Because the potentially large radiation losses caused by this contamination have a strong Z (atomic number) dependence, low-Z materials are desirable for limiters or other first-wall elements. Low-Z coatings offer the promise of separating the functions of impurity control and structural requirements.

It has also been shown that the first-wall provides an appreciable part of the fueling in tokamaks due to the release of hydrogen which has accumulated on (or in) the first-wall from prior discharges.[3] It is therefore important for plasma considerations to determine the hydrogen recycle characteristics of candidate coating materials.

In the future, although structural, plasma contamination, and hydrogen recycle requirements will remain imperative, emphasis will most certainly shift to include the question of tritium inventory control. Indeed, this is already of great concern in the design of proposed tokamaks, e.g., TFTR. In this regard, the evaporation of Ti to control plasma refueling may lead to unacceptably large tritium inventories. Thus, with the approach of the era of D-T burning tokamaks, comprehensive questions on the behavior of H isotopes (T in particular) in first-wall materials must be answered.

A particularly important feature that has been observed in previous studies[4-7] of hydrogen trapping in metals (e.g., W, Au, Pd, Mo, and Nb) is the enhanced trapping of hydrogen in the near surface region due to the presence of damage. This damage can be produced rather efficiently by the implantation of helium or other ions. It is, therefore, important to understand the

synergistic or interactive effects of radiation damage and the trapping of excess hydrogen in the near-surface region of fusion first-wall materials.

The direct exposure of samples in an operating tokamak provides a rigorous check on conclusions drawn from implantation studies to simulate plasma-wall interactions. Si, C, and stainless steel 304 surfaces have been exposed and analyzed for H profile and H saturation characteristics. In addition, these measurements have lead to the development of a diagnostic technique to determine the fluence and energy spectra of escaping H isotopes.

The present paper briefly reviews previous results for the ion-induced damage trapping of hydrogen in the near surfaces of metals and tokamak exposure studies. Current results are reviewed on the trapping, release, and He damage assisted retention of hydrogen in CVD-deposited TiB_2 coatings and bulk B_4C samples that are under development for high-power tokamak surfaces.

II. EXPERIMENTAL

Hydrogen isotopes, as well as a variety of damaging ions have been implanted into the near surface regions of samples using ion accelerators, operating below 100 kV. In the previous studies for molybdenum and niobium,[7] <100>-oriented single crystals were used. Smooth, damage-free surfaces were prepared by mechanical lapping, followed by electropolishing for molybdenum and chemical polishing for niobium. The implantation energies for the predamage ions were chosen to maintain the ion damage deposition within the

first approximately 100 Å of the surface. The hydrogen injection energy was chosen to have an ion range near the middle of the damage deposition regions. Ion energies used were 11 and 18 keV $^4He^+$, 55-keV Ne^+, 55-keV O^+, 500-keV Bi^+, and 16-keV H_2^+ to obtain 8-keV H ions, and 16-keV D_2^+ to obtain 8-keV D ions. The nuclear reaction $D(^3He,p)^4He$ was used for measuring the total amount of D retained within the near surface region. The analyzing ^3He beam was obtained from a 2-MeV Van de Graaff at approximately 750 keV, giving a probing depth of about 0.5 microns. A solid state detector with a solid angle of 0.1 sr was placed at an angle of approximately 130° with respect to the incident beam and detected the 13 MeV protons coming from the nuclear reaction.

Depth profiles of the H retained in the targets were measured by means of a ^{19}F beam from a tandem accelerator. The nuclear reaction $^1H(^{19}F,\alpha\gamma)^{16}O$ was used. This technique has been described in detail previously.[8,9] The main feature as illustrated in Fig. 1, is the use of a very sharp peak or resonance in the energy dependence of the nuclear reaction cross section. By changing the incident beam energy, the depth at which the resonance occurs is changed, and by measuring the gamma yield from the reaction with a sodium-iodide scintillation counter as a function of incident F energy, one can obtain the depth profile of the hydrogen. The stopping power values tabulated by Anderson and Ziegler[10] were used to convert the fluorine energy scale to a depth scale.

Two candidate first-wall materials, TiB_2 and B_4C, were examined. The TiB_2 samples were thin (~50 μm) CVD coatings on POCO graphite substrate;[11] whereas, the B_4C samples were hot pressed and in bulk form.[12] B_4C has been used as a limiter material in TFR 400[13] and behaved satisfactorily up to discharge currents of 80 kA, but failed at higher currents due to thermal shock. Although TiB_2 has yet to be tested on a limiter, simulation results on thin coatings are very promising.[14] TiB_2-coated limiters will be tested on ISX-B later this year. B_4C coatings are also under investigation with the hope that these coatings will not be as sensitive to thermal shock as is bulk B_4C.

III. IMPLANTATION PROFILES AND RELEASE TEMPERATURES

Knowledge of the temperature at which H is released from a candidate material is necessary to permit prediction of recycling behavior and to anticipate problems relating to the control of tritium inventories. In order to measure the temperature at which hydrogen is released from TiB_2 and B_4C, ^1H was implanted (60 keV for TiB_2, 30 keV for B_4C) to depths of 3000 - 4000 Å, and the samples were annealed isochronally for 20 minutes at increasing temperatures. ^1H profiles were measured between each anneal, and these profiles along with plots of H retention as a function of anneal temperature are shown in Fig. 2. Clearly, H is retained in B_4C to much higher temperatures than in TiB_2. One-half of the H in TiB_2 is released by 400°C, whereas, 700°C

is required for the same fractional release in B_4C. The relative constancy of the width of the H peak as a function of temperature indicates that the release is trap-limited in both materials. This observation indicates that the implanted H is trapped in its own ion-induced damage.

In previous reports,[15-17] approximate H trap energies in TiB_2 were deduced from the isochronal anneal data by assuming no subsequent retrapping of H once it was liberated. This assumption, however, may not be valid because retrapping in He-induced damage has been directly observed[17] and is reported later in this paper. Trap energies listed in our earlier works should therefore be considered as upper limits.

IV. DAMAGE TRAPPING

Since molybdenum and niobium diffusion studies[18] indicate that hydrogen isotopes are mobile at room temperatures, the previous measurements[4-7] of the retention of hydrogen isotopes in the near surface region indicated that trapping occurs. Large enhancements in the amounts of deuterium retained over samples without prior predamage were observed. For a given predamage ion fluence, the deuterium retention increased linearly with deuterium fluence until a saturation level was reached. Above saturation fluence, almost the same fraction of additional deuterium ions incident on the target were retained in the predamaged and nondamaged samples. That is, above the saturation level, the slopes of the D retention versus D fluence are the

same for both cases. For most metals without predamage the concentration of trapped hydrogen was too low to obtain well-defined depth profiles, but with helium predamage the hydrogen depth profile clearly depended on the predamaging helium-ion energy, and concentrations of hydrogen up to 10 at.% were observed as shown in Fig. 3.

Hydrogen-defect trapping rather than hydrogen-impurity trapping is indicated since no chemical effects of the predamage ion species were observed for oxygen and neon predamaging ions in molybdenum. In addition, too many hydrogen atoms were found to be trapped per incident damaging ion to be explained simply by impurity trapping. For example, in the case of neon, as many as 40 deuterium atoms were observed to be trapped for each incident predamaging neon ion. In the previous experiments, the predamaging ion energy was chosen to deposit its damaging energy into depths less than 1000 $\mathring{A}$, and the hydrogen injection energy was chosen such that the hydrogen slowed to rest within this region. Also, the most efficient trapping per number of primary displacements was found to occur for helium ions with decreasing efficiencies as the predamaging ion mass was increased to neon or to bismuth. An extended tail of hydrogen to deeper depths was always observed in the case of bismuth, neon, or oxygen damage.

In annealing studies of neon predamaged molybdenum[7] the release of hydrogen from traps was found to occur around 200°C (50% loss for 10-minute anneal). This corresponded to the

release of hydrogen from the traps rather than the annealing of the traps, since a predamaged sample annealed to 300°C prior to hydrogen introduction gave the same total trapping as observed for the non-annealed sample. In molybdenum, this relatively high temperature for release implies that the combined hydrogen binding plus migration energy is large (~1.5 eV) and this contrasts to much lower binding energies of about 0.2 to 0.3 eV which were reported for hydrogen trapped at dislocations and disorder induced by cold working in other bcc metals.

The present results for TiB_2 give measurements of the effects of helium predamage on hydrogen trapping in a non-metal. Titanium-diboride is a very stable, refractory with a melting temperature of ~ 2900°C. It has high thermal conductivity, low thermal expansion, and, as a result, good resistance to thermal stresses. It is an extremely hard material, and its hardness is not as temperature dependent as most other refractories. TiB_2 has good chemical resistance, particularly at high temperatures, and has better oxidation resistance than carbides and nitrides. The samples were deposited by CVD at 950°C and x-ray studies showed they were stoichiometric TiB_2.

Figure 4 shows the depth profiles of 60 keV 10^{17} H/cm^2 implanted into titanium-diboride coatings which have been predamaged with 30 keV 10^{17} He/cm^2. The profile at 400°C shows the definite decoration of the helium damage profile by the hydrogen as it is moving toward the surface. This result, and measurements after high-temperature anneals, show

that the hydrogen traps in the helium damage are more stable than traps created by the hydrogen self-implantation damage. These measurements are the first to show the redistribution of hydrogen from the as-implanted depth distribution to the helium trapping distribution during annealing. In the previous measurements in metals the hydrogen was mobile at the temperature of implantation and was directly implanted into the helium predamaged region. Therefore, the hydrogen moved and decorated the damage prior to the profile measurements. Experiments are now in progress to determine the stability of the helium-induced hydrogen traps.

In Fig. 5 we show the profiles of the hydrogen trapping at a 400°C annealing temperature for three predamage helium fluences. Increasing the helium predamage fluence increases the hydrogen trapping in the helium predamage region. For both this figure and Fig. 4 the projected range of 60 keV H ions has been normalized to the centroid of the as-implanted H profile to obtain the depth scale. The abscissa mark labeled "30 keV He" corresponds to the depth of the maximum in the damage distribution caused by 30 keV He ions on TiB_2 as calculated by Brice to be 1300 Å.

In addition, the effects on H retention of 80 and 140 keV He predamage has been investigated and the resulting H profiles are shown in Fig. 6. The 30, 80, and 140 keV He implants ($10^{17}/cm^2$) result in damage distributions which peak at 1300, 3030, and 4740 Å into the sample, respectively. After the He was injected, H was implanted at 60 keV (3200 Å) to a fluence of $10^{17}/cm^2$ and

then the samples were annealed in an argon atmosphere at 400°C for 20 minutes. Decoration of the He-produced damage can be seen for the 30 and perhaps the 80 keV He implant but is not observed for the 140 keV He implant. This observation is consistent with the predominance of surface directed H migration during the anneal. At present we have no clear understanding why H should preferentially diffuse toward the surface, although a possible explanation may be that the asymmetric near-surface self-damage of the H ions during implantation creates a preferential diffusion path toward the surface. A similar study on B_4C has been performed and in this case H decoration of deeper He predamage is observed, which indicates that H appears to undergo a more isotropic diffusion in B_4C than the surface-directed motion observed in TiB_2.

The TiB_2 samples were also subjected to 20 min isochronal anneals at 400, 500, and 600°C and the H retention is plotted in Fig. 7 as a function of the depth of the predamage peak for the three anneal temperatures. The dotted lines in this figure are eye-guides. The peaked behavior of the isotherms at 400 and 500°C indicates that damage retrapping is most efficient when there is a maximum overlap between the damaged and the initial implant (~0.3 μm) region. This, however, does not appear to be the case for the 600°C anneal. For comparison, when no He is preinjected, the relative amount of H retained in the TiB_2 sample was 57, 16, and 4% following 400, 500, and 600°C anneals, respectively. This retention is much lower than that

measured for predamaged samples. Therefore, if a high H retention is required of a first-wall material, e.g., to minimize recycle, predamaging by ion implantation may be considered as a controlled processing step. Predamage, however, may not be necessary since the first wall will naturally be subjected to a flux of energetic ions during discharges and, hence, this surface may become sufficiently damaged after an initial break-in period to retain H more efficiently than the virgin undamaged material.

Another concern is the use of a coating for a high-power surface is whether H or its isotopes, particularly T, will accumulate at the coating-substrate interface. This build-up could reduce adhesion and, as mentioned above, is of environmental concern. To test for this build-up, thin TiB_2 coatings were CVD deposited onto polished (1 μ diamond paste) POCO graphite disks. The coating thickness was measured by Rutherford backscattering analysis using a 3 MeV He^+ beam and was found to be 1.2 ± 0.1 μm. The uncertainty is not experimental but, instead, indicates the nonuniformity of the coating thickness. H was implanted at 220 keV (∿1 μm) to a fluence of $2 \times 10^{17}/cm^2$. The resulting H profiles both before and after a 400°C, 20-minute anneal are shown in Fig. 8. Note the suppressed zero for the depth scale. The ∿1.5 at.% concentration of H in the POCO graphite is natural and presumably occurs during its production. That virgin POCO graphite contains appreciable hydrogen has been verified in a separate experiment where an H profile was measured for a virgin sample. From the two profiles shown in the figure, it is clear that no H accumulation is occurring at the interface.

V. PULSED ANNEALING

One problem with the use of thermal annealing to purge H from first walls is that support structures, mainly stainless steel components, will also undergo temperature elevation. Such temperatures may not be desirable because of fatigue considerations, due to the high temperatures (> 400 C for TiB_2) required for significant H (or T) release. Removal of first-wall elements (i.e., limiters, armor plating, channel walls) for H desorption external to the tokamak is one way to circumvent the problem; however, the handling of tritium-loaded components is not an attractive prospect.

Another, more novel, approach is the use of pulsed electron or laser annealing. Because pulsed annealing concentrates heat only in the near surface region, underlying structures remain unaffected. In situ H purging would therefore be plausible.

Electron beam annealing of TiB_2 coatings implanted with 10^{17} cm^{-2}, 60 keV H ions was performed with an 0.8 sec pulse of 0.3 A/cm^2, 8 keV electrons. The effect of the anneal is demonstrated by the H profiles in Fig. 9 and shows that complete H release has obviously been accomplished. Although the anneal temperature was not monitored, heat transport calculations suggest a peak surface temperature of ~ 2400 C. Air thermal annealing measurements have shown that a significant H purging can be accomplished at much lower temperatures and, hence, an electron beam of reduced power density may accomplish the same dramatic effect.

We have also laser annealed H-implanted (60 keV, $10^{17}/cm^2$) TiB_2 coatings with a Q-switched Nd:glass laser which produces a

25 ns pulse of 1.06 μm wavelength light. Energy densities of 1.75 J/cm^2 were used. The resulting H profiles following 0, 1, and 3 1.5 J/cm^2 pulses are shown in Fig. 10. The H profiles following single laser pulses of 1.5 or 1.75 J/cm^2 were nearly identical, which suggests that at 1.5 J/cm^2 a melt or energy deposition depth of ~ 3000 Å (the implant depth) is achieved. Approximately 40% of the H in the coating is released following each laser shot.

Pulsed laser annealing of H-implanted B_4C was also investigated. Figure 11 gives a comparison of the H retention for both TiB_2 and B_4C as a function of the number of laser pulses. In part (a) of the figure the incident energy was 1.5 J/cm^2 and in part (b) this energy was doubled.

VI. SAMPLE EXPOSURES IN TOKAMAKS

The dramatic improvement in plasma operating conditions obtained by Ti gettering has demonstrated the significance of H recycling on tokamak operation. A complementary technique to implantation for investigation of the H recycle behavior of fusion materials is the direct exposure of samples at the edge of an operating tokamak. In this case the "implantation" which results from the escape of energetic hydrogen from plasma, is generally characterized by a Maxwellian energy distribution with characteristic energy less than 500 eV. Relatively few hydrogen trapping studies have been carried out at such low energies.

Figure 12 shows an example of the D depth profile as measured by the D(^{3}He, α)^{1}H nuclear reaction for Si and stainless steel surfaces exposed for a long period of time (two months operation and ~10^3 high power discharges) in the PLT tokamak. The difference in the nature of the trapping is clearly exhibited by the depth profiles. In both Si and stainless steel the D is believed to be mobile at room temperature and the D is immobilized by subsequent trapping. In stainless steel the D is trapped in a surface layer, presumably due to the natural oxide and a carbon contaminant carbonaceous layer deposited during operation. However in Si the D is distributed in depth, presumably due to bulk defect trapping of the D. Saturation concentrations are typically reached at ~ 30 at.% after which any additional hydrogen injected escapes back out through the surface.

Bulk trapping allows a much greater reservoir of hydrogen to be built up for subsequent recycle than does surface trapping. Similar bulk trapping behavior to that of Si has recently been observed for C and is expected from the laboratory studies of TiD_2 and B_4C. An important aspect of combined laboratory and tokamak implantation studies is the ability to draw correlations, thereby further establishing the mechanisms involved and providing a basis for inferring hydrogen recycle characteristics at the plasma edge from laboratory implantation studies.

An additional recent benefit of sample exposure studies in tokamaks has been their use as a plasma edge diagnostic. From the observed trapping of hydrogen in C or Si as a function of

number of discharges and a knowledge of the retention trapping behavior it has been possible to determine the hydrogen flux as a function of distance from the plasma. In addition the depth distribution of the hydrogen can be used to determine the characteristic Maxwellian energy at which the particles reach the probe. Results have recently been reported for a wide high power discharges in PLT operation without auxiliary heating. Fluences range from 10^{16}-10^{17}/cm^2 per discharge and characteristic energies (which includes the sheath potential) range from 100-400 eV, in both cases decreasing with increasing distance from the plasma. Such studies are valuable in that they provide a quantitative basis for estimating such impurity effects as energy flow to limiters, impurity release due to sputtering and hydrogen recycling.

VII. SUMMARY

In summary, ion implantation and ion microanalysis are providing important information on plasma-surface interaction in fusion devices.

References

1. Princeton University Plasma Physics Laboratory Publication PH-N-009, 1978.

2. P. Staib and G. Staudenmaier, J. Nucl. Mater. 76/77, 78 (1978).

3. G. M. McCracken, J. Nucl. Mater. (in press).

4. G. M. McCracken and S. K. Erents, Applications of Ion Beams to Materials, ed. G. T. Picraux, E. P. EerNisse, and F. L. Vook (Plenum Press, New York, 1974) p. 585.

5. S. T. Picraux and F. L. Vook, J. Nucl. Mater. 53, 246 (1974).

6. S. T. Picraux, J. Bøttiger, and N. Rud, Appl. Phys. Lett. 28, 179 (1976); J. Nucl. Mater. 63, 110 (1976).

7. J. Bøttiger, S. T. Picraux, N. Rud, and T. Laursen, J. Appl. Phys. 48, 920 (1977).

8. J. Bøttiger, J. R. Leslie, and N. Rud, J. Appl. Phys. 48, 1672 (1976).

9. D. A. Leich and T. A. Tombrello, Nucl. Instr. Methods 108, 67 (1972).

10. H. H. Anderson and J. F. Ziegler, Hydrogen Stopping Powers and Ranges in All Elements, (Pergamon Press, NY, 1977).

11. H. O. Pierson, E. Randich, and D. M. Mattox, J. of Less Common Metals (in press).

12. Norton Company, Industrial Ceramics Division, Worcester, MA, 01606.

13. TFR Group, EUR-CEA-FC-852, October 1976.

14. D. M. Mattox, A. W. Mullendore, H. O. Pierson, J. Nucl. Mater. (in press).

15. B. L. Doyle and F. L. Vook, J. Nucl. Mater. (in press).

16. B. L. Doyle and F. L. Vook, Nucl. Sci. Trans., NS-26, 1305 (1979).

17. F. L. Vook, B. L. Doyle, and S. T. Picraux, Nucl. Sci. Trans., NS-26, 1272 (1979).

15. J. Völkl and G. Alefeld, Diffusion in Solids, (Academic Press, NY, 1975), p. 321; H. T. Stalnaker and C. A. Wert, Ber. Bunsenges. Phys. Chem. 76, 806 (1972); R. E. Stickney, The Chemistry of Fusion Technology, ed. D. M. Gruen (Plenum Press, NY, 1972) p. 241.

Figure Captions

Fig. 1 ^{1}H profiling schematic. By changing the incident energy of the ^{19}F beam, the sharp energy resonance is swept in depth, and the γ yield gives the H concentration in depth.

Fig. 2 ^{1}H profiles and retention curves for B_4C and TiB_2 after annealing. Boxes b. and d. show the ^{1}H profiles as measured by nuclear reaction analysis for ^{1}H implanted into B_4C and TiB_2, respectively. These samples were annealed isochronally at the indicated temperatures. The profiles have been displaced vertically for clarity. Boxes a. and c. show the respective retention curves for B_4C and TiB_2.

Fig. 3 H profiles in Mo after room temperature He predamage and subsequent 8 keV H implantation to 1×10^{17} cm^{-2}. Arrows indicate projected ranges for the He predamaging ions.

Fig. 4 H profiles of H implanted (10^{17} cm^{-2}, 60 keV), He predamaged (10^{17} cm^{-2}, 30 keV) TiB_2 after 20-minute anneals at the indicated temperature. Surface at left.

Fig. 5 H profiles after 20-minute, 400°C anneals for the indicated 30 keV He predamage fluences.

Fig. 6 H profiles of 60 keV-10^{17} H/cm^2 implantation, 10^{17} He/cm^2 predamaged TiB_2 after a 20-minute 400°C anneal.

Fig. 7 H retention of 60 keV-10^{17} H/cm^2 implanted TiB_2 plotted as a function of 10^{17} He/cm^2 predamage depth and 20-minute anneal temperature.

Fig. 8 H profiles of 210 keV-2 x 10^{17} H/cm^2 implanted TiB_2 (1.2 μm) on POCO graphite before and after a 20-minute 400°C anneal.

Fig. 9 H profiles of 60 keV-10^{17} H/cm^2 implanted TiB_2, before and after exposure to pulsed electron beam anneal (6 keV, 0.3 A/cm^2, 0.8 sec).

Fig. 10 H profiles of 60 keV-10^{17} H/cm^2 implanted TiB_2, A: As implanted, B: After one laser pulse, C: After two more pulses. Laser pulse parameters: 20 ns, 1 μm, 1.5 J/cm^2.

Fig. 11 H retention in B_4C and TiB_2 after annealing with a Q-switched Nd:glass laser ($\lambda \sim 1$ μm, $\tau \sim 20$ ns). In box a. the energy flux was 1.5 J/cm^2 while in box b. it was 3.0 J/cm^2.

Fig. 12 Deuterium retention and profiling for samples exposed in PLT.

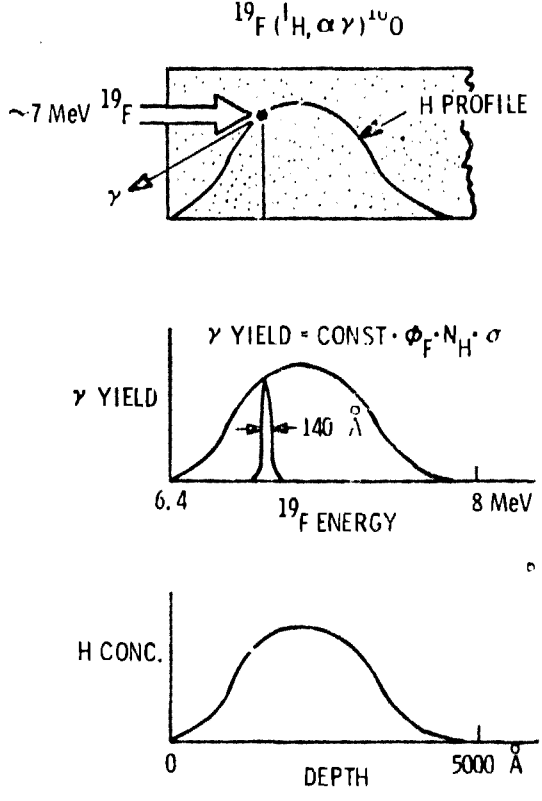
$^{19}F(^{1}H,\alpha\gamma)^{16}O$
~7 MeV ^{19}F
H PROFILE
γ
γ YIELD = CONST · $\phi_F \cdot N_H \cdot \sigma$
γ YIELD
140 Å
6.4
^{19}F ENERGY
8 MeV
H CONC.
0
DEPTH
5000 Å

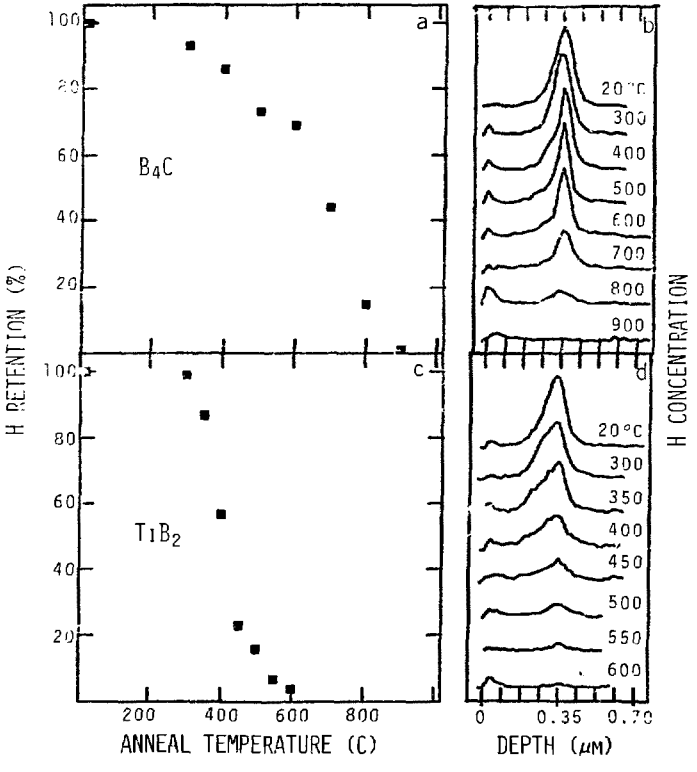
a
b
c
d
B_4C
TiB_2
H RETENTION (%)
H CONCENTRATION
ANNEAL TEMPERATURE (C)
DEPTH (μM)
20°C
300
400
500
600
700
800
900
20°C
300
350
400
450
500
550
600
0
0.35
0.70
200
400
600
800

Figure 1

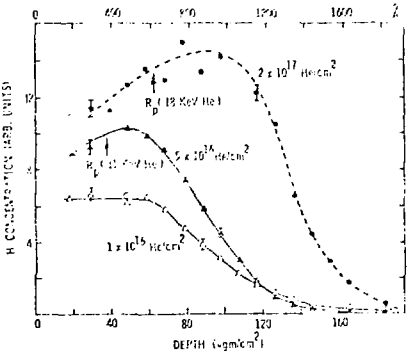

Figure 3

H PROFILES OF 30 KEV He (10^{17}/CM^2) PREDAMAGED TiB$_2$

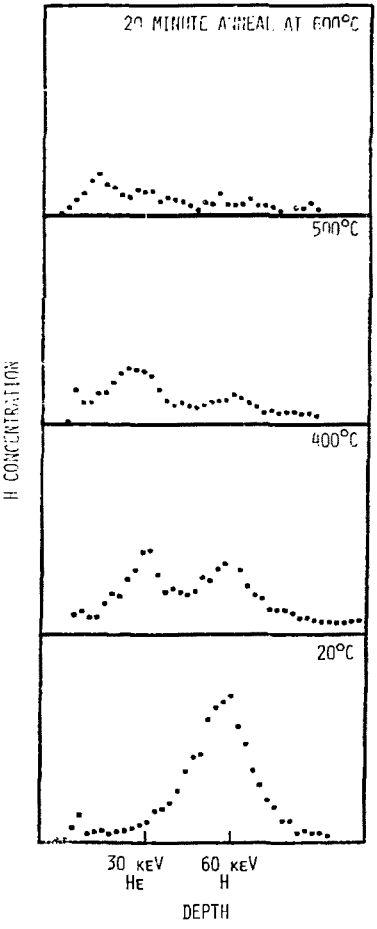

H PROFILES OF
30 KEV HE PREDAMAGED TiB_2
ANNEALED AT 400°C

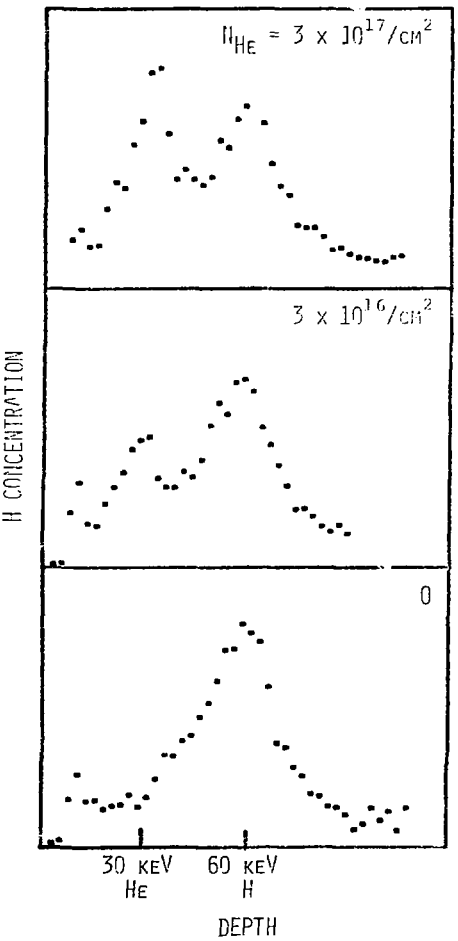

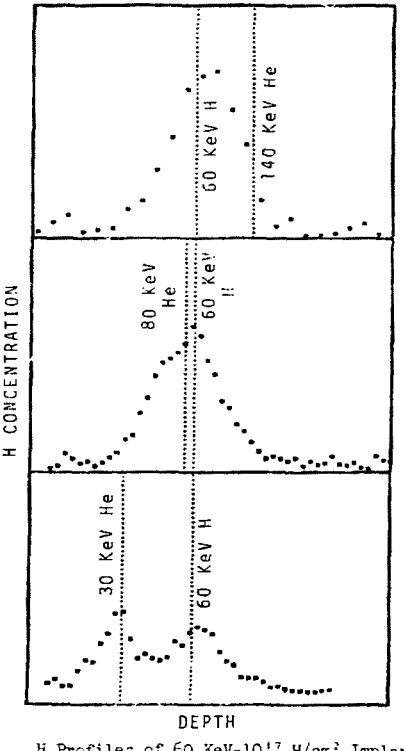

H Profiles of 60 KeV-10^{17} H/cm^2 Implanted, 10^{17} He/cm^2 Predamaged TiB_2 After a 20 Minute 400°C Anneal.

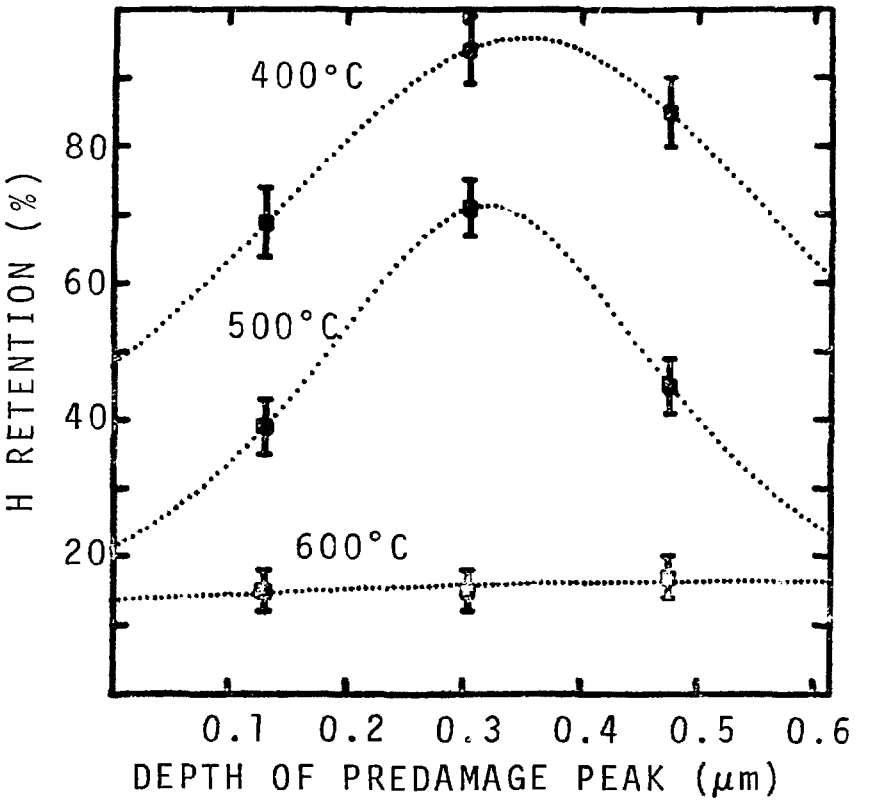

H Retention of 60 KeV-10^{17} H/cm^2 Implanted TiB_2 Plotted as a Function of 10^{17} He/cm^2 Predamage Depth and 20 Minute Anneal Temperature.

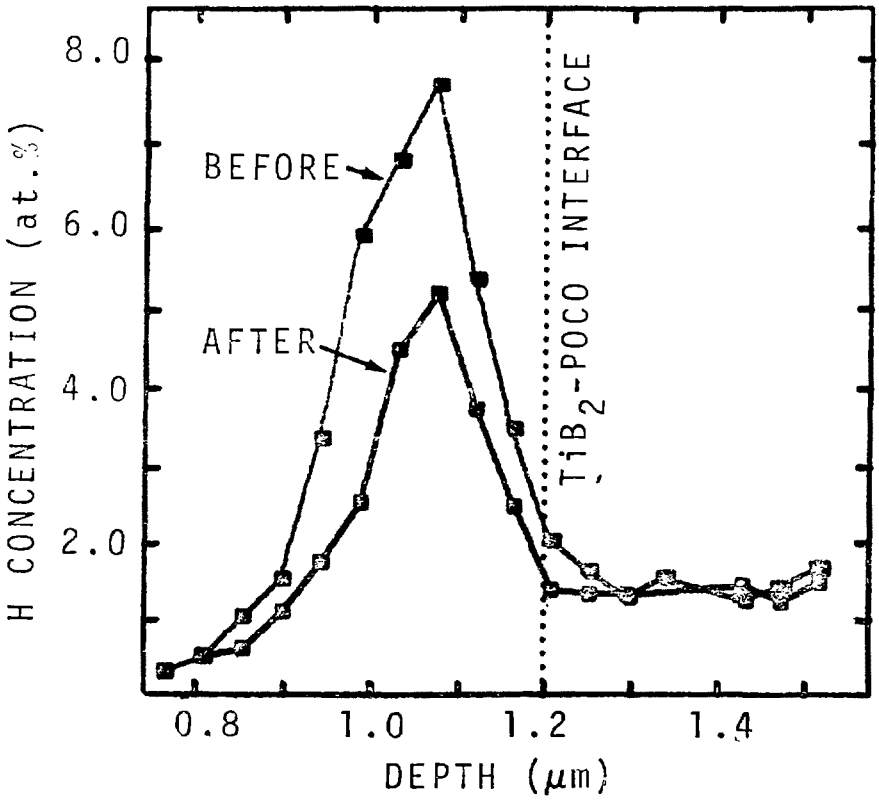

H Profiles of 210 KeV-2 x 10^{17} H/cm^2 Implanted TiB_2 (1.2 μm) on POCO Graphite Before and After 20 Minute 400°C Anneal.

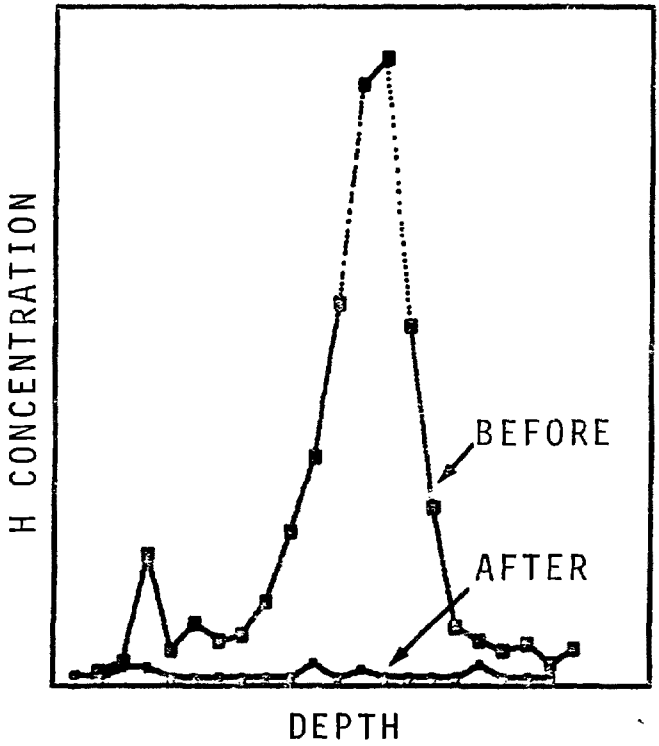

H Profiles of 60 KeV-10^{17} H/cm^2 Implanted TiB_2, Before and After Exposure to Pulsed Electron Beam Anneal (8 KeV, .3 A/cm^2, .8 sec).

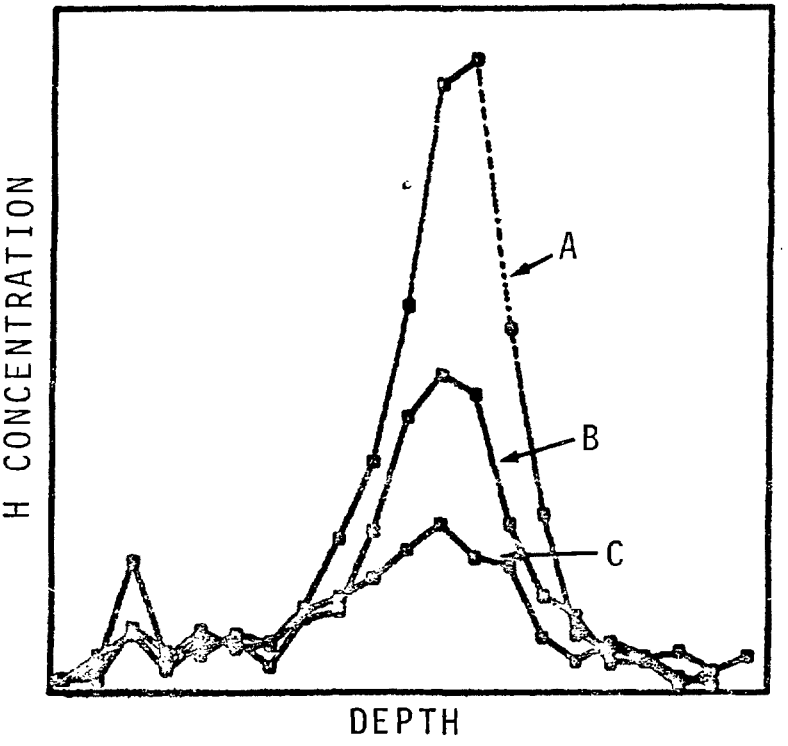

H Profiles of 60 KeV-10^{17} H/cm^2 Implanted TiB_2, A: As Implanted, B: After One Laser Pulse, C: After Two More Pulses. Laser Pulse Parameters: 20 ns, 1 μm, 1.5 J/cm^2.

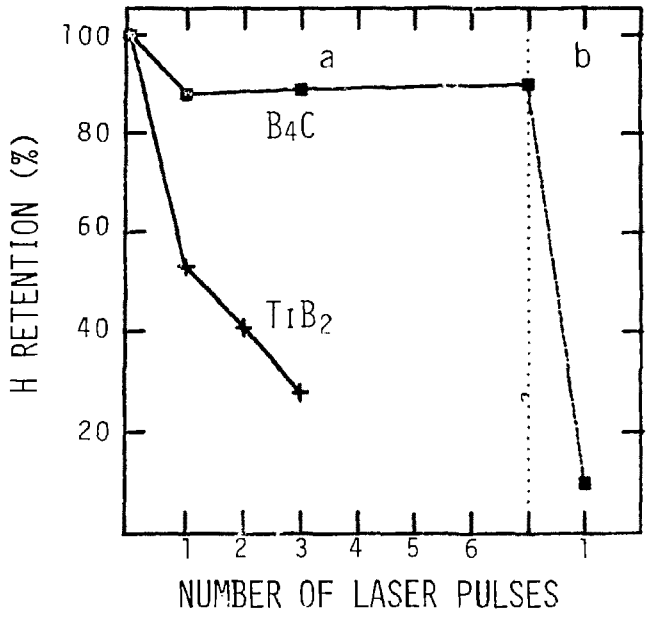
100
80
60
40
20
H RETENTION (%)
a
b
B4C
TiB2
1
2
3
4
5
6
1
NUMBER OF LASER PULSES

Figure 3

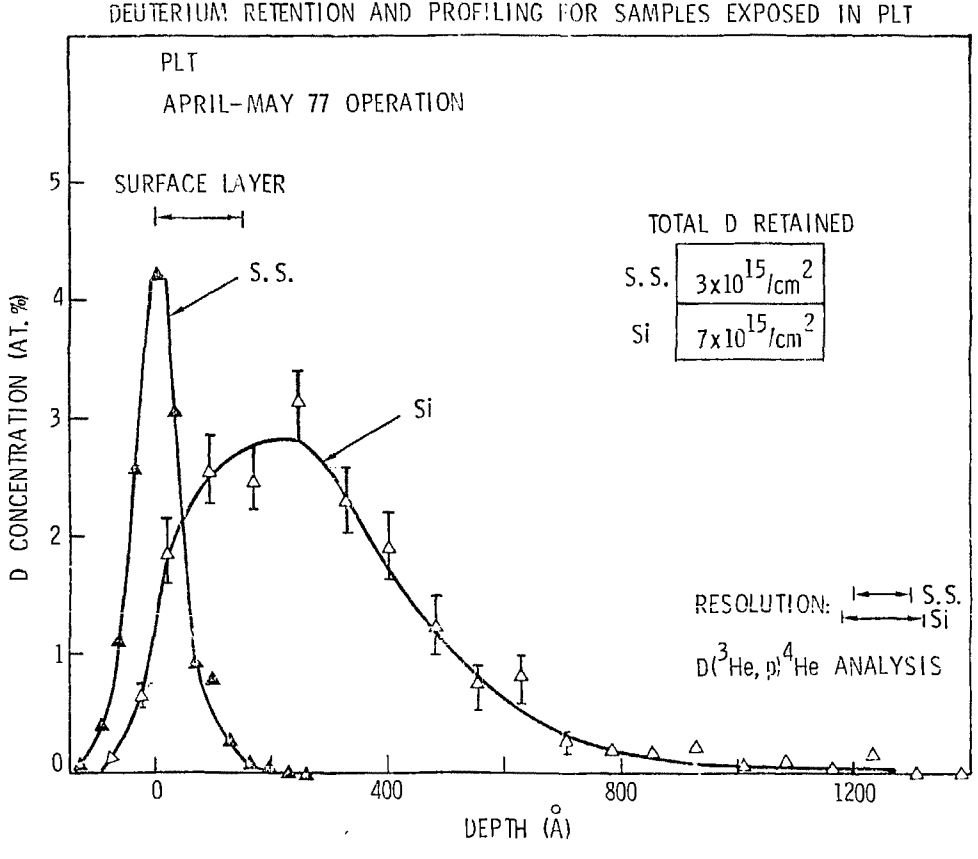
DEUTERIUM RETENTION AND PROFILING FOR SAMPLES EXPOSED IN PLT
PLT
APRIL-MAY 77 OPERATION
SURFACE LAYER
S.S.
Si
TOTAL D RETAINED
S.S. 3x10^15/cm^2
Si 7x10^15/cm^2
RESOLUTION: S.S. Si
D(3He, p)4He ANALYSIS
D CONCENTRATION (AT. %)
DEPTH (Å)
0
1
2
3
4
5
0
400
800
1200